

## Dynamic fluorescence changes during photodynamic therapy *in vivo* and *in vitro* of hydrophilic Al(III) phthalocyanine tetrasulphonate and lipophilic Zn(II) phthalocyanine administered in liposomes

Angelika Rück <sup>a,\*</sup>, Gerd Beck <sup>a</sup>, Rüdiger Bachor <sup>b</sup>, Nermin Akgün <sup>a</sup>, Michael H. Gschwend <sup>a</sup>, Rudolf Steiner <sup>a</sup>

<sup>a</sup> Institut für Lasertechnologien in der Medizin und Meßtechnik, Helmholtzstraße 12, D-89081 Ulm, Germany

<sup>b</sup> Urologische Universitätsklinik, Pritzwitzstraße 43, D-89075 Ulm, Germany

### Abstract

The fluorescence emission of hydrophilic tetrasulphonated aluminium phthalocyanine (AlPcS<sub>4</sub>) and hydrophobic zinc phthalocyanine (ZnPc), bound to the membrane of liposomes, was investigated *in vivo* in an appropriate tumour model of the rat bladder and in RR 1022 epithelial cells of the rat. The sensitizers were administered systemically to the rats and photodynamic therapy (PDT) was performed 24 h later. During PDT treatment, the fluorescence was measured every 30 s. The fluorescence was excited with 633 nm light from an HeNe laser and the fluorescence spectra were detected with an optical multichannel analyser system. PDT was performed for both sensitizers using 672 nm light from an Ar<sup>+</sup> dye laser.

The fluorescence changes during PDT were significantly different for the two phthalocyanines. For AlPcS<sub>4</sub>, an initial fluorescence intensity increase, followed by subsequent photobleaching, was observed. In contrast, ZnPc fluorescence showed an exponential decrease and no increase at the start of treatment. Tumour necrosis 24 h after PDT was significant only for ZnPc.

RR 1022 cells incubated for 24 h with AlPcS<sub>4</sub> revealed a granular fluorescence pattern, whereas ZnPc was localized diffusely in the cytoplasm of the cells. In agreement with the *in vivo* measurements, subcellular relocalization and a fluorescence intensity increase were detected exclusively in the case of AlPcS<sub>4</sub>. Morphological changes at this time were significant only for ZnPc. The subcellular localization and fluorescence kinetics were obtained using a confocal laser scanning microscope.

**Keywords:** Cell culture; Fluorescence kinetics; Fluorescence spectroscopy; Hydrophilic AlPcS<sub>4</sub>; Liposomal ZnPc; Lysosomes; Photobleaching; Photodynamic therapy; Rat bladder tumour model; Relocalization

### 1. Introduction

Several new classes of photosensitizers have been suggested in recent years for photodynamic therapy (PDT). Of these, phthalocyanines (Pcs) have received considerable interest [1,2]. As a result, the photochemistry, photobiology and photodynamic efficiency of Pcs have been studied in detail [3,4]. Most biological studies have been conducted with water-soluble metallo-Pcs. In addition, the hydrophobic, non-sulphonated, zinc(II) phthalocyanine (ZnPc) has been incorporated into the membranes of liposomes [5]. The pharmacological properties of liposomally delivered ZnPc and the low sensitizer dose needed to obtain a satisfactory tumour reduction after PDT treatment make this drug a promising candidate for PDT [6].

It is well known that the localization of a sensitizer in tumour cells influences to some extent the photodynamic activity. The cellular distribution is certainly determined by the uptake mechanism, which is mainly influenced by the composition of the medium and the use of carrier systems. Most of the hydrophilic photosensitizers are taken up by pinocytosis and accumulate in extranuclear granules, as observed for sulphonated aluminium phthalocyanines [7]. Uptake via the low density lipoprotein (LDL) endocytotic pathway has been demonstrated for liposomally administered sensitizers [8]; thus a final accumulation in the lysosomal membrane can be the result.

The intracellular location can change with time [9]. This phenomenon, which is characterized as relocation or redistribution, is important because the location within the cell affects the efficiency of PDT. This has been demonstrated on a poorly differentiated squamous cell carcinoma [10]. Pho-

\* Corresponding author.

tofrin II (PII) was incubated in the cells and the rates of sensitizer uptake and redistribution were correlated with the PDT efficiency.

Relocation of sensitizers is observed not only during the incubation time, but also during PDT treatment [11,12]. The light-induced reactions depend on the subcellular localization of the dye. Interestingly, hydrophilic dyes, which finally accumulate in large amounts in storage organelles, are re-localized during PDT, sometimes correlating with fluorescence intensity increases and spectral changes [13]. However, the contribution of relocalization to the overall PDT effect is still under discussion.

In this paper, we report on the dynamic fluorescence changes of hydrophilic tetrasulphonated aluminium phthalocyanine (AlPcS<sub>4</sub>) and hydrophobic ZnPc administered in liposomes. Fluorescence spectroscopy during PDT treatment was investigated *in vivo* in a rat bladder tumour model. Light-induced subcellular relocalization and dynamic fluorescence changes were observed in parallel in cell culture using laser scanning microscopy.

## 2. Materials and methods

### 2.1. Chemicals

Liposomally delivered ZnPc (CGP 55 847) was obtained from Ciba-Geigy (Basel, Switzerland) and injected intravenously at a concentration of 0.3 mg (kg body weight)<sup>-1</sup> into the animals. For the subcellular localization studies, cells were incubated with 10<sup>-5</sup> M ZnPc.

Hydrophilic AlPcS<sub>4</sub> was obtained from the Russian Academy of Sciences, General Physics Institute, Moscow, Russia. Stock solutions of the sensitizer were made up in phosphate-buffered saline (PBS) and sterilized by filtration using a 0.2 µm filter. The dye was injected intravenously into the animals and applied at a concentration of 5 mg (kg body weight)<sup>-1</sup>. In parallel, cell cultures were incubated with 10<sup>-5</sup> M AlPcS<sub>4</sub> for the study of subcellular light-induced reactions.

### 2.2. Cell cultures

Cultures of epithelial cells from the rat (RR 1022, ATCC No. CCL47) were grown in Dulbecco's modified Eagle's medium (DMEM) supplemented with 10% foetal calf serum (FCS) and antibiotics at 37 °C and 5% CO<sub>2</sub>. For microscopic investigations, the cells were cultured on microscope slides; 25 cells mm<sup>-2</sup> were seeded 24 h before incubation with the sensitizers. The medium was removed and the cells were incubated for another 24 h with 10<sup>-5</sup> M AlPcS<sub>4</sub> or 10<sup>-5</sup> M ZnPc (DMEM, 5% FCS, 37 °C, 5% CO<sub>2</sub>). The incubation period coincided with the late lag phase and the early growth phase [14]. The microscopic experiments were performed immediately after removing the incubation medium and rinsing twice with PBS.

### 2.3. Tumour model

AY 27 cells, originating from a chemically induced bladder carcinoma of Fischer CDF rats, were injected at the cranial site into the bladder of Fischer CDF rats. During injection of the cell suspension, the animals were anaesthetized. After 7 days of tumour growth, the sensitizers were injected intravenously at the concentrations mentioned above. PDT was performed 24 h after administration of the photosensitizer. The tumour was irradiated with 672 nm light for AlPcS<sub>4</sub> and ZnPc. The total irradiation was 25 J cm<sup>-2</sup> (ignoring the integrating sphere effect of the bladder). PDT effectiveness was observed as tumour necrosis, which was evaluated histologically 24 h after PDT treatment.

### 2.4. Experimental set-up for *in vivo* irradiation and fluorescence spectroscopy

During intrabladder irradiation and fluorescence spectroscopy, the animals were generally anaesthetized and the bladder was filled with saline to give a final sphere with a mean diameter of approximately 11 mm. The experimental set-up is shown in Fig. 1. Two fibres were placed through the channel of a catheter into the bladder. The excitation fibre with an isotropic diffuser at the end was adjusted into the centre of the bladder. Fluorescence excitation was performed with an HeNe laser (633 nm) and PDT irradiation with light from an Ar<sup>+</sup> dye laser. For both fluorescence excitation and therapy, the light was transmitted by the same fibre. During PDT treatment, every 30 s the light path from the Ar<sup>+</sup> dye laser was interrupted with a shutter and the fluorescence emission spectrum was measured. The fluorescence intensity was detected with the second fibre adjusted to an optical multi-channel analyser system (Biospec, Moscow). The control of the measurements and the calculation of the fluorescence spectra were performed with the program MOSA.2. The detection fibre was fixed independently from the excitation fibre for maximum fluorescence intensity. A cut-off filter in front of the CCD camera minimized the backscattered HeNe light. It was ensured that, during PDT treatment and fluorescence spectroscopy, the position of the fibres did not change.

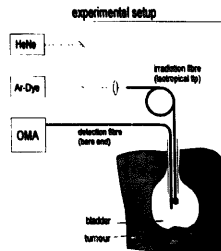


Fig. 1. Experimental set-up for intrabladder PDT and fluorescence spectroscopy (for details see text).

Fluorescence spectra during PDT treatment were recorded for ten animals for both photosensitizers. Three animals, which received no photosensitizer, served as controls. The dosimetry of the PDT light was calculated to give a power density of  $80 \text{ mW cm}^{-2}$  (ignoring the integrating sphere effect of the bladder). The transmitted power of the HeNe laser was  $4 \text{ mW}$ .

## 2.5. Fluorescence microscopy

The subcellular localization of the photosensitizers and the dynamic fluorescence changes during light exposure were evaluated using a laser scanning microscope (LSM 410 invert, Zeiss, Germany). Confocal fluorescence images were obtained by exciting the cells with an internal HeNe laser ( $633 \text{ nm}$ ), with detection of the fluorescence above  $665 \text{ nm}$  with a photomultiplier (beam splitter FT  $655 \text{ nm}$ , long-pass filter RG  $665 \text{ nm}$ ). The fluorescence distribution was recorded with the red channel of the microscope. Simultaneously, the phase contrast images were detected with the green channel. The scanning time for one image was  $1 \text{ s}$ . A  $40\times$  magnification phase contrast objective lens (aperture,  $0.75 \text{ mm}$ ) was used together with a zoom factor of three to five.

The subcellular fluorescence patterns of the sensitizers were detected before and every second within a  $79 \text{ s}$  irradiation time of the scanning laser beam. Because of the scanning mode, the exact dosimetry is not easy to calculate; however, approximately  $0.2 \text{ J cm}^{-2}$  was applied every second to the monolayer; thus a total irradiation dose of  $16.3 \text{ J cm}^{-2}$  was delivered to the cells. Image processing software was used for the registration of the time series. The subcellular fluorescence kinetics during light-induced treatment were calculated in the case of AIPcS<sub>4</sub> in a special defined region of interest (ROI).

## 3. Results

### 3.1. Fluorescence spectroscopy during light-induced reactions *in vivo*

Fig. 2 shows the fluorescence emission spectra of AIPcS<sub>4</sub> observed from the bladder tumour of the animal. The fluorescence was excited at  $633 \text{ nm}$ , as described in Section 2. PDT treatment was performed with  $672 \text{ nm}$  light. The fluorescence emission spectrum reveals a main peak at  $690 \text{ nm}$ . The peak at  $633 \text{ nm}$  is due to the remaining transmittance from the HeNe laser. During PDT, the fluorescence spectrum was recorded every  $30 \text{ s}$ . After  $30 \text{ s}$  of irradiation, which corresponds to a light dose of  $2.5 \text{ J cm}^{-2}$ , the fluorescence intensity is increased by a factor of two as shown in Fig. 2. After a higher light dose, the fluorescence intensity decreases. The intensity after the total administered light dose ( $25 \text{ J cm}^{-2}$ ,  $300 \text{ s}$  irradiation) is approximately the same as before PDT treatment. Although the reflectance does not remain

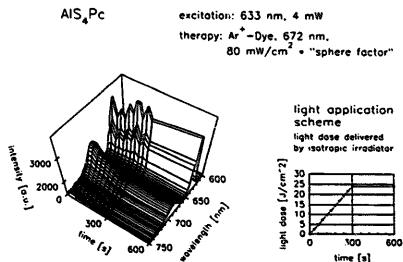


Fig. 2. Fluorescence kinetics of AIPcS<sub>4</sub> during intrablander irradiation.

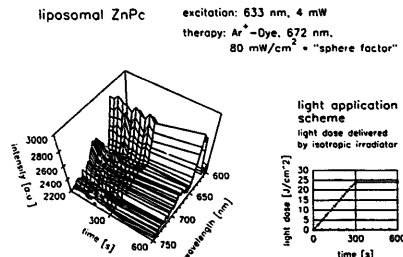


Fig. 3. Fluorescence kinetics of liposomal ZnPc during intrablander irradiation.

constant during PDT treatment, the initial fluorescence increase is reproducible and is observed in all cases of ten treated rats. Control animals, which received no sensitizer, show autofluorescence in the red spectral region and no fluorescence modifications during light exposure.

Fig. 3 shows the fluorescence emission spectra of liposomally administered ZnPc in the bladder of rats. The fluorescence was again excited at  $633 \text{ nm}$  and PDT treatment was performed at  $672 \text{ nm}$ . The main fluorescence band is blue shifted by about  $8 \text{ nm}$  compared with that of AIPcS<sub>4</sub>. The fluorescence spectra were again recorded every  $30 \text{ s}$  during PDT. Interestingly, a similar fluorescence intensity increase at the start of treatment is not observed. During light exposure, the fluorescence intensity decreases exponentially. This effect is again reproducible for the ten treated rats. As demonstrated in Fig. 3, the reflectance at  $633 \text{ nm}$  does not remain constant during PDT treatment.

Tumour necrosis, which was evaluated histologically  $24 \text{ h}$  after PDT treatment, was significant in the case of ZnPc [15]. However, rats treated with AIPcS<sub>4</sub> did not show significant tumour necrosis  $24 \text{ h}$  after PDT. In both cases, the normal bladder epithelium remained intact.

### 3.2. Dynamic fluorescence changes *in vitro* during light-induced reactions

Fig. 4(a) shows the subcellular localization of AIPcS<sub>4</sub> in RR 1022 cells (after  $24 \text{ h}$  incubation). The green channel of

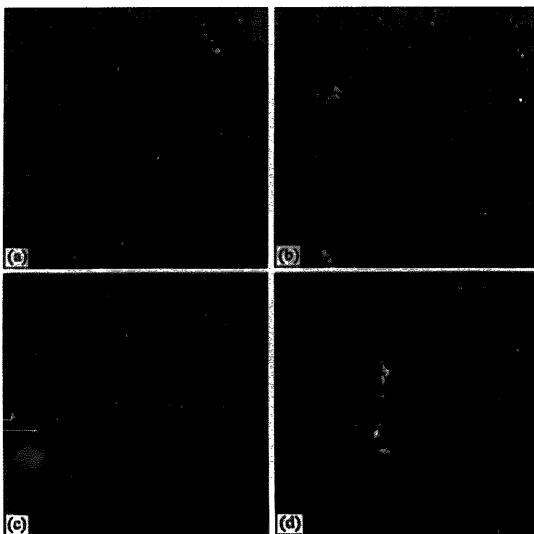


Fig. 4. (a) Subcellular fluorescence of AIPcS<sub>4</sub> in RR 1022 cells before PDT. Cells were incubated for 24 h with  $10^{-5}$  M AIPcS<sub>4</sub>. Green channel, phase contrast; red channel, fluorescence. (b) Subcellular fluorescence of AIPcS<sub>4</sub> in RR 1022 cells after  $5.1 \text{ J cm}^{-2}$  of irradiation (for details see (a)). (c) Subcellular fluorescence of liposomal ZnPc in RR 1022 cells before PDT. Cells were incubated 24 h with  $10^{-5}$  M ZnPc. (d) Subcellular fluorescence of liposomal ZnPc in RR 1022 cells after  $5.1 \text{ J cm}^{-2}$  irradiation.

the LSM was taken for the phase contrast image of the cells and the red channel for fluorescence localization (for excitation and detection, see Section 2). Before PDT, the subcellular fluorescence of AIPcS<sub>4</sub> is correlated with extranuclear granules localized predominantly at one site of the cytoplasm in the vicinity of the nucleus. During PDT with 633 nm light, the fluorescence intensity is markedly increased at the start of treatment (Fig. 4(b), after  $5.1 \text{ J cm}^{-2}$  of irradiation), similar to our recent observations [16]. At this time, morphological changes are only marginal and predominantly observed at the cytoplasmic level. Some vacuoles and granules disappear and the nucleus becomes pycnotic. As demonstrated by sections along the optical axis (*z* direction), fluorescence formation in the nucleus is not observed.

For a detailed observation of the subcellular fluorescence changes, a ROI was defined in the vicinity of the nucleus and the images were detected every second (after  $0.2 \text{ J cm}^{-2}$  of irradiation) during PDT. This is demonstrated in Fig. 5 and the corresponding fluorescence kinetics are given in Fig. 6. The initial fast fluorescence intensity increase, which reaches a maximum after  $5.1 \text{ J cm}^{-2}$  of irradiation (25 s), is followed by a subsequent photobleaching process. We conclude that at least two processes are responsible for the dynamic behaviour of AIPcS<sub>4</sub>. After the totally administered light dose of  $16.3 \text{ J cm}^{-2}$  (79 s of irradiation), significant cell damage at

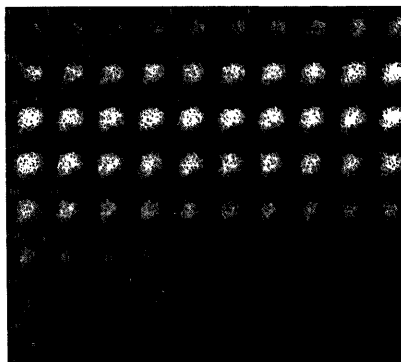


Fig. 5. Subcellular fluorescence changes of AIPcS<sub>4</sub> in RR 1022 cells in the vicinity of the nucleus (ROI). Images were detected every second (after  $0.2 \text{ J cm}^{-2}$  of irradiation).

the plasma membrane, such as bubbles and blebs, can be observed (data not shown).

In the case of liposomally administered ZnPc, the sensitizer is distributed more diffusely in the cytoplasm. In addition,

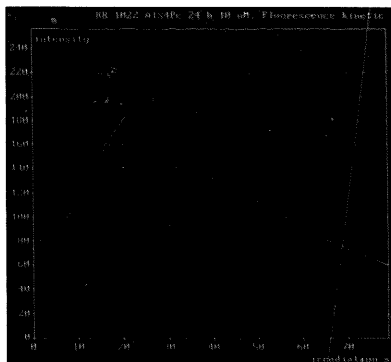


Fig. 6. Subcellular fluorescence kinetics of AlPcS<sub>4</sub> in RR 1022 cells in the vicinity of the nucleus. Fluorescence intensity corresponds to Fig. 5.

some fluorescent granules are observed. This is demonstrated in Fig. 4(c). During light exposure, the fluorescence completely disappears (Fig. 4(d), after  $5.1 \text{ J cm}^{-2}$  of irradiation). An initial fluorescence intensity increase and relocalization are not observed. Compared with AlPcS<sub>4</sub>, morphological changes after  $5.1 \text{ J cm}^{-2}$  of irradiation are more significant, especially at the membrane level (see Fig. 4(d)). Interestingly, this enhanced PDT effect corresponds to the findings *in vivo*.

#### 4. Discussion

In this work, we present the detection of the light-induced reactions of two phthalocyanines which differ significantly in their hydrophobicity/lipophilicity. The highly hydrophilic AlPcS<sub>4</sub> and lipophilic ZnPc administered in liposomes were investigated in cell cultures and in a rat bladder tumour model. It is well known that cellular light-induced reactions are dependent on the subcellular localization of the photosensitizer. Photobleaching in the sense of photodegradation is observed for hydrophobic sensitizers such as protoporphyrin IX (PPIX), although the intermediate formation of photo-products can be detected [17,18]. As main intracellular targets, the plasma membrane, nucleus, mitochondria and lysosomes have been identified for these compounds [19,20].

It has been shown in this work that ZnPc fluorescence, which is distributed diffusely at the subcellular level in the cytoplasm 24 h after incubation, is photobleached monotonously during light exposure. This phenomenon, which was also observed *in vivo*, confirms the photobleaching behaviour of other hydrophobic sensitizers, thus indicating the binding of ZnPc to membrane structures (perhaps lysosomes and mitochondria), which are probably the main targets. The

evaluation of tumour necrosis showed a significant PDT effect 24 h after treatment, although 100% necrosis was not obtained for all animals [15].

The PDT effect of ZnPc on the vasculature and tumour cells has been reported in the literature [21]. *In vivo* fluorescence and photodynamic activity were investigated using a skinfold chamber rat model with a transplanted mammary carcinoma. Approximately the same amount of fluorescence in the tumour and blood vessels 24 h after injection of the sensitizer could be detected. As outlined in Ref. [21], tumour control by PDT with liposomal ZnPc therefore requires vascular damage; therefore the endothelium is probably a target as well as the tumour cells.

In contrast with hydrophobic sensitizers, hydrophilic dyes, which accumulate inside extranuclear granules, can be relocalized during PDT. This has been shown for lysosomotropic dyes, such as meso-tetra(4-sulphonatophenyl)porphyrin (TPPS<sub>4</sub>) [11,12] and Nile blue [22], and was confirmed for AlPcS<sub>4</sub> and AlPcS<sub>2</sub> [7,16] (see, in addition, Fig. 4(a) and Fig. 4(b)). From Fig. 4(a), it is evident that AlPcS<sub>4</sub> reveals a granular fluorescence distribution in a discrete perinuclear region. This was also deduced for AlPcS<sub>2</sub> incubated in leukaemic K 562 cells [23]. In Ref. [23], the localization was associated with lysosomes. During irradiation, fluorescence redistribution and subsequent monomerization of the dye are correlated with changes in the fluorescence decay from a biexponential to a monoexponential behaviour [23]. In addition, time-gated microspectrofluorometry indicates changes in the fluorescence emission spectra [13]. In association with relocalization, a new fluorescence band appears, which is blue shifted by about 30 nm from the main fluorescence peak, and selectively detected between an early time gate.

From Fig. 2 and Fig. 6, it can be seen that, after the initial fluorescence intensity increase, the fluorescence subsequently decreases. It should be noted that the fluorescence increase of AlPcS<sub>4</sub> in the rat bladder has been detected, to our knowledge, for the first time in an appropriate *in vivo* model. In the literature, photobleaching in the normal rat bladder wall, especially in the deeper muscle, has been reported [24]. Our measurements show that, after a light dose at which the fluorescence intensity is at a maximum *in vitro* ( $5.1 \text{ J cm}^{-2}$ ), no significant morphological changes can be observed with light microscopy (Fig. 4(b)). In addition, the induced tumour necrosis is only minimal 24 h after PDT treatment with a total light dose of  $25 \text{ J cm}^{-2}$ .

The initial fluorescence intensity increase of AlPcS<sub>4</sub> *in vivo* and *in vitro* raises the question of whether this is due to a release of the dye from extranuclear granules such as endosomes or lysosomes with or without rupture of the organelles. Subcellular relocalization due to release is evident from our cell culture experiment; however, the situation *in vivo* may be more complex. In addition to subcellular changes, dye exchange between the various cell types of tumour tissue can influence the fluorescence signal even during PDT. Moreover, the contribution of lysosomal damage during PDT to the overall cell killing effect is still controversial. Experiments

with cells in different growth states, incubated with TPPS<sub>4</sub>, indicated loss of membrane integrity in growing cells as well as in stationary cells, although lysosomal release of the dye was only observed in growing cells [14].

Lysosomal damage seems to be important for lipophilic dyes which induce permeation of the lysosomal membranes. In this case, release of acidic hydrolases into the cytoplasm [25] or release of the lysosomal enzymes  $\beta$ -N-acetyl-D-glucosaminidase ( $\beta$ -AGA) and cathepsin (L + B) [26] can be observed, enzymes which are supposed to contribute to the killing effect. However, hydrophilic dyes, which are accumulated in large amounts in lysosomes, are involved in the almost complete inactivation of these enzymes, observed in the case of TPPS<sub>4</sub> [26] and AlPcS<sub>4</sub> [27]. A small light dose, which causes redistribution of AlPcS<sub>4</sub> accompanied by a more than tenfold increase in the fluorescence quantum yield, inactivates the enzymes  $\beta$ -AGA and cathepsin (L + B) [27]. As reported in Ref. [27], such small light doses are almost non-toxic for the cells. Subsequent photodegradation after the tenfold fluorescence increase is practically non-existent and redistribution does not result in any significant increase in the photosensitivity of the cells [27]. In contrast, we observed, after relocation and the initial fluorescence increase of AlPcS<sub>4</sub>, subsequent photobleaching correlated with morphological damage at the plasma membrane. Nevertheless, the PDT efficiency in our rat bladder model was only marginal with this sensitizer. Possible reasons may be that relocation does not induce an increase in the photosensitivity or the mechanisms *in vivo* are more complex. Moreover, as recently reported, the most efficient wavelength for PDT in the case of sulfonated hydrophilic Pcs can be red shifted *in vivo* as well as in cell culture by 10–15 nm [28,29].

## 5. Conclusions

We can conclude that lipophilic ZnPc administered in liposomes induces significant tumour necrosis and cell damage after PDT treatment and this correlates with the photobleaching behaviour of the sensitizer. The damage of membrane structures seems to be evident. In contrast, AlPcS<sub>4</sub> reveals a more complex situation. Relocalization of the photosensitizer is the first step during PDT, followed by subsequent photobleaching. However, only in the case of cell cultures can damage of the cells be observed; the induction of tumour necrosis failed. Thus it is questionable whether the photobleaching process in the case of AlPcS<sub>4</sub> is necessarily correlated with effective damage, probably at the membrane structures of the cells. Another explanation for the low phototoxicity *in vivo* may be the choice of irradiation wavelength, which probably differs from the optimum absorption maximum of the sensitizer *in vivo*. Moreover, our results confirm reports in the literature which favour lipophilic over hydrophilic dyes with respect to the induction of tumour necrosis [30].

## Acknowledgements

This work was supported in part by the Deutsche Forschungsgemeinschaft. Gerd Beck is a scholar of Evangelisches Studienwerk Villigst, D-58239 Schwerte). The authors wish to thank Felicitas Genze for technical assistance with the animals.

## References

- [1] J.E. van Lier and J.D. Spikes, The chemistry, photophysics and photosensitizing properties of phthalocyanines, in G. Bock and S. Harlett (eds.), *Photosensitizing Compounds: Their Chemistry, Biology and Clinical Use, Ciba Foundation Symposium 146*, Wiley, Chichester, 1989, pp. 17–32.
- [2] E. Ben-Hur, Photochemistry and photobiology of phthalocyanines: new sensitizers for photodynamic therapy of cancer, in A. Favre et al. (eds.), *From Photophysics to Photobiology*, Elsevier Science, New York, 1987, pp. 407–420.
- [3] E. Ben-Hur, Basic photobiology and mechanisms of action of phthalocyanines, in T.J. Dougherty and B.W. Henderson (eds.), *Photodynamic Therapy: Basic Principles and Clinical Applications*, Marcel Dekker, New York, 1991, pp. 63–77.
- [4] P.J.O. Nuutinen, P.T. Chattani, J. Beöweli, A.J. MacRobert, D. Phillips and S.G. Bown, Distribution and photodynamic effect of disulfonated aluminium phthalocyanine in the pancreas and adjacent tissues in the Syrian golden hamster, *Br. J. Cancer*, **64** (1991) 1108–1115.
- [5] G. Valduga, E. Reddi, G. Jori, R. Cubeddu, P. Taroni and G. Valentini, Steady state and time-resolved spectroscopic studies on zinc(II) phthalocyanine in liposomes, *J. Photochem. Photobiol. B: Biol.*, **16** (1992) 331–340.
- [6] K. Schieweck, H.-G. Capraro, U. Isele, P. van Hoogevest, M. Ochsner, T. Maurer and E. Blatt, CPG 55 847, liposome-delivered zinc(II)-phthalocyanine as a phototherapeutic agent for tumors, *SPIE Proc.*, **2078** (1994) 107–118.
- [7] Q. Peng, G.W. Farrants, K. Madslien, J.C. Bommer, J. Moan, H.E. Danielsen and J.M. Nesland, Subcellular localization, redistribution and photobleaching of sulfonated aluminum phthalocyanines in a human melanoma cell line, *Int. J. Cancer*, **49** (1991) 290–295.
- [8] G. Jori and E. Reddi, The role of lipoproteins in the delivery of tumor-targeting photosensitizers, *Int. J. Biochem.*, **25** (1993) 1369–1375.
- [9] H. Schneckeburger, A. Rück, B. Bartos and R. Steiner, Intracellular distribution of photosensitizing porphyrins measured by video-enhanced fluorescence microscopy, *J. Photochem. Photobiol. B: Biol.*, **2** (1988) 355–363.
- [10] X.Y. He, S.L. Jacques and G. Gofstein, Effectiveness of photosensitive dye during uptake and redistribution. Optical methods for tumor treatment and detection, *SPIE Proc.*, **1645** (1992) 205–215.
- [11] K. Berg, K. Madslien, J.C. Bommer, R. Oftebro, J.W. Winkelman and J. Moan, Light induced relocalization of sulfonated meso-tetrahydroporphyrins in NIH3T3 cells and effects of dose fractionation, *Photochem. Photobiol.*, **53** (1991) 203–210.
- [12] A. Rück, T. Köllner, A. Dietrich, W. Strauß and H. Schneckeburger, Fluorescence formation during photodynamic therapy in the nucleus of cells incubated with cationic and anionic water-soluble photosensitizers, *J. Photochem. Photobiol. B: Biol.*, **12** (1992) 403–412.
- [13] A. Rück, H. Schneckeburger, W. Strauß, M. Gschwend and R. Steiner, Intracellular relocalization of anionic photosensitizers measured by cw and time-gated microscopy and spectroscopy. Optical and imaging techniques in biomedicine, *SPIE Proc.*, **2329** (1994) 244–251.

- [14] W.S.L. Strauss, M.H. Gschwend, R. Sailer, H. Schneckenburger, R. Steiner and A. Rück, Intracellular fluorescence behaviour of meso-tetra(4-sulphonatophenyl)porphyrin during photodynamic treatment at various growth phases of cultured cells, *J. Photochem. Photobiol. B: Biol.*, **28** (1995) 155–161.
- [15] R. Bachor et al., in preparation.
- [16] A. Rück, C. Hildebrandt, T. Köllner, H. Schneckenburger and R. Steiner, Competition between photobleaching and fluorescence intensity increase of photosensitizing porphyrins and tetrasulphonated chloroaluminiumphthalocyanine, *J. Photochem. Photobiol. B: Biol.*, **5** (1990) 311–319.
- [17] J. Moan and D. Kessel, Photoproduct formed from photofrin II in cells, *J. Photochem. Photobiol. B: Biol.*, **1** (1988) 429–436.
- [18] K. König, H. Schneckenburger, A. Rück and R. Steiner, In vivo photoproduct formation during PDT with ALA-induced endogenous porphyrins, *J. Photochem. Photobiol. B: Biol.*, **18** (1993) 287–290.
- [19] R. Santus and P. Morliere, The photobiology of the living cell as studied by microspectrofluorometric techniques, *Photochem. Photobiol.*, **54** (1991) 1071–1077.
- [20] M. Geze, P. Morliere, J.C. Maziere, K.M. Smith and R. Santus, Lysosomes as key target of hydrophobic photosensitizers proposed for phototherapeutic applications, *J. Photochem. Photobiol. B: Biol.*, **20** (1993) 23–35.
- [21] H.L.L.M. van Leengoed, V. Cuomo, A.A.C. Versteeg, N. van der Veen, G. Jori and W.M. Star, In vivo fluorescence and photodynamic activity of zinc phthalocyanine administered in liposomes, *Br. J. Cancer*, **69** (1994) 840–845.
- [22] C.-W. Lin, J.R. Shulok, S.D. Kirley, C.M. Bachelder, T.J. Flotte, M.E. Sherwood, L. Cincotta and J.W. Foley, Photodynamic destruction of lysosomes mediated by nile blue photosensitizers, *Photochem. Photobiol.*, **58** (1993) 81–91.
- [23] M. Ambroz, A.J. MacRobert, J. Morgan, G. Rumbles, M.S.C. Foley and D. Phillips, Time-resolved fluorescence spectroscopy and intracellular imaging of disulphonated aluminium phthalocyanine, *J. Photochem. Photobiol. B: Biol.*, **22** (1994) 105–117.
- [24] A.J. Poje, A.J. MacRobert, D. Phillips and S.G. Bown, The detection of phthalocyanine fluorescence in normal rat bladder wall using sensitive digital imaging microscopy, *Br. J. Cancer*, **64** (1991) 875–879.
- [25] P. Morliere, E. Kohen, J.P. Reyftmann, R. Santus, C. Kohen, J.C. Maziere, S. Goldstein, W.F. Mangel and L. Dubertret, Photosensitization by porphyrins delivered to L cell fibroblasts. A microspectrofluorometric study, *Photochem. Photobiol.*, **46** (1937) 183–191.
- [26] K. Berg and J. Moan, Lysosomes as photochemical targets, *Int. J. Cancer*, **59** (1994) 1–9.
- [27] J. Moan, K. Berg, H. Anholt and K. Madslien, Sulfonated aluminium phthalocyanines as sensitizers for photochemotherapy. Effects of small light doses on localization, dye fluorescence and photosensitivity in V79 cells, *Int. J. Cancer*, **58** (1994) 865–870.
- [28] J. Griffiths, J. Cruse-Sawyer, S.R. Wood, J. Schofield, S.B. Brown and B. Dixon, On the photodynamic therapy action spectrum of zinc phthalocyanine tetrasulphonic acid in vivo, *J. Photochem. Photobiol. B: Biol.*, **24** (1994) 195–199.
- [29] G. Canti, D. Lattuada, E. Leroy, R. Cubeddu, P. Taroni and G. Valentini, Action spectrum of photoactivated phthalocyanine AIS<sub>2</sub>Pc in tumor bearing mice, *Anticancer Drugs*, **3** (1992) 139–142.
- [30] H.L.L.M. van Leengoed, N. van der Veen, A.A.C. Versteeg, R. Quillet, J.E. van Lier and W.M. Star, In vivo photodynamic effects of phthalocyanines in a skin-fold observation chamber model: role of central metal ion and degree of sulphonation, *Photochem. Photobiol.*, **58** (1993) 575–580.